Development of an ion CT system based on 4D-tracking and time-of-flight based residual energy determination

LLU workshop 2021, 3^{rd} of August, 2021

Felix Ulrich-Pur on behalf of the protonCT group at HEPHY/TU Wien

HEPHY
INSTITUT FÜR HOCHENERGIEPHYSIK

TU WIEN
TECHNISCHE UNIVERSITÄT WIEN

Outline

HEPHY INSTITUT FÜR HOCHENERGIEPHYSIK

TU WIEN TECHNISCHE UNIVERSITÄT WIEN

Motivation – Replacement of old pCT demonstrator

Project status

- Current pCT demonstrator was build from existing hardware (Ulrich-Pur et al. 2021)
  - Double-sided Si-strip detectors
  - TERA range telescope
  - Huge development efforts had to be made to get demonstrator operational
- Performance was measured at MedAustron
  - RSP accuracy ≈ 0.59 %
  - RSP resolution ≈ 9.3 %
  - Mean DAQ rate ≈ 0.9 kHz
- Not designed for clinical use
  - Establish pCT workflow

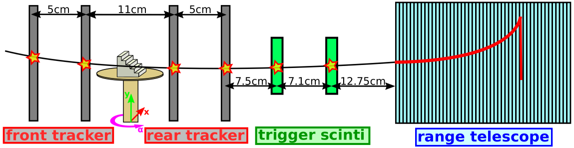

Experimental setup

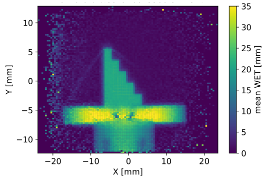

Forward projection

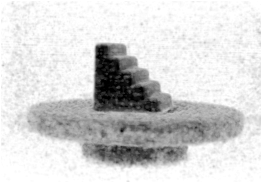

3D RSP map

HEPHY INSTITUT FÜR HOCHENERGIEPHYSIK
TU WIEN TECHNISCHE UNIVERSITÄT WIEN

Overview – iCT system based on 4D-tracking detectors

Next step: upgrade solution based on 4D tracking detectors

- Simulataneous measurement of particle position and time
- Residual energy is estimated via time-of-flight measurement
  - No need to stop particles in calorimeter
- TOF through object can be used for particle identification (filtering) (Rovituso et al. 2017)
- Strong interest from HEP to develop fast 4D tracking detectors with high granularity (Sadrozinski et al. 2017)

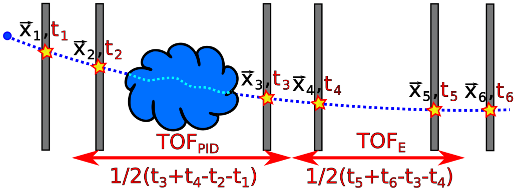

Ion computed tomography setup based on 4D tracking detectors

Overview – Low Gain Avalanche Detector

Full iCT system solely based on Low Gain Avalanche Detectors (LGADs)

- Intrinsic gain layer with controlled gain ($\approx$ 10-30) improves SNR and time resolution
  - High time resolution ($30 - 50\,\text{ps}$) (Pietraszko et al. 2020, Pitters et al. 2020)
- Short rise times ($\mathcal{O}(1\,\text{ns})$)
- Small pitch (spatial resolution $< 100\,\mu$m) vs fill factor
- Low material budget ($X/X_0 << 1\,\%$ for strips)

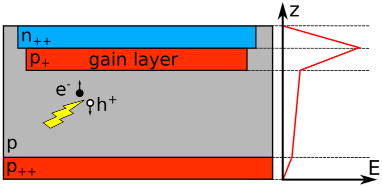

Low Gain Avalanche Detector

$$\sigma_t{}^2 \approx \underbrace{\left(\frac{t_{\text{rise}}}{\text{SNR}}\right)^2}_{\approx\sigma^2_{\text{jitter}}} + \underbrace{\sigma_{t,\text{floor}}{}^2}_{\text{gain indep.}}$$

Intrinsic time resolution (Sadrozinski et al. 2017)

Outline

TOF calorimeter – Overview

Residual energy calculation via time-of-flight measurements

- Influence of system parameters on energy resolution and accuracy was studied
- Simulation of different detector technologies (pixel, strip)
  - $\frac{X}{X_0} = 0.1\text{-}2.3\,\%$ (Si+dielectric(FR4)+Cu compound)
- Assumptions for the energy measurement
  - Straight line track
  - No energy loss inside calorimeter

$$E_{\text{kin}} = m_0 c^2 \cdot \left(\frac{1}{\sqrt{1 - \frac{L^2}{c^2 \text{TOF}^2}}} - 1 \right)$$

- Development of calibration procedure required

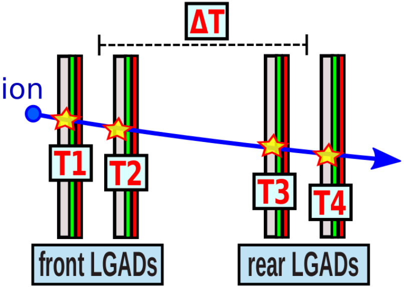

LGAD based TOF calorimeter

TOF calorimeter – Energy resolution (precision)

Theoretical energy resolution of a TOF calorimeter

- Intrinsic TOF resolution should be $\leq 30\,\text{ps}$ per plane to achieve Eres $< 1\,\%$ (goal for WEPL detector) (Bashkirov et al. 2016)
  - In general : $\sigma_{\text{WET}} \propto \frac{\sigma_{\text{E}_{\text{resid}}}}{S_W(\text{E}_{\text{resid}})}$ (Collins-Fekete et al. 2020)

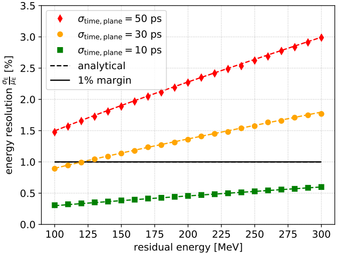

L=1m, $\frac{X}{X_0} = 0.1\,\%$

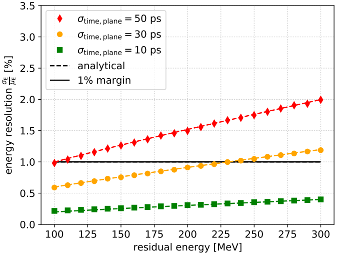

L=1.5 m, $\frac{X}{X_0} = 0.1\,\%$

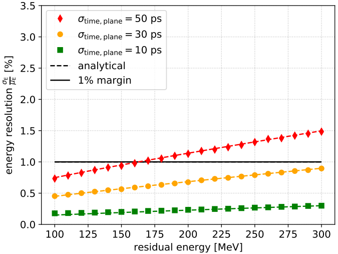

L=2m, $\frac{X}{X_0} = 0.1\,\%$

$$\frac{\sigma_{E_{kin}}}{E_{kin}} = \frac{\gamma^3\beta^2}{L(\gamma-1)}\sqrt{\sigma_{\text{TOF}}{}^2\beta^2c^2 + \sigma_L{}^2}$$ with $\sigma_{\text{TOF}} = \sqrt{\frac{2}{n}}\sigma_{\text{time,plane}}$

TOF calorimeter – Calibration (accuracy)

Systematic error I

- Particles loose energy along path which increases TOF
  - Energy is underestimated

$$\mathrm{TOF} = \int_0^L \frac{\mathrm{d}s}{v(\vec{x}(s))} \neq \frac{L}{v_{\mathrm{residual}}}$$

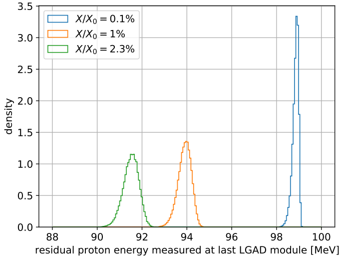

Impact of energy loss along flightpath: 100 MeV **protons,** 0.5 m **flightpath**

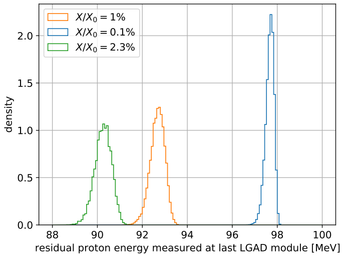

Impact of energy loss along flightpath: 100 MeV **protons,** 2 m **flightpath**

TOF calorimeter – Calibration (accuracy)

Systematic error II

- Symmetric total TOF distribution (with σ_{TOF}) leads to an asymmetric residual energy distribution (E-TOF relationship)
  - Shift towards lower energies
  - Increases for higher energies and higher σ_{TOF}

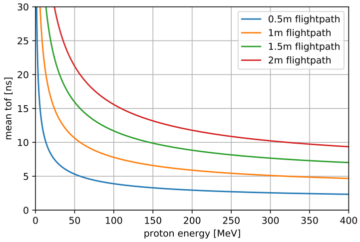

Time-of-flight for different beam energies

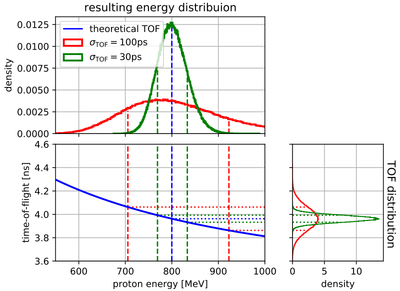

Asymmetric shift of energy distribution due to non-linear E-TOF relation

TOF calorimeter – Calibration (accuracy)

- Absolute error is dominated by material budget (energy loss)
  - Flight distance not as significant as material budget (energy loss in air is almost negligible)
- Intrinsic time resolution $\sigma_{\mathrm{time,plane}}$ is more dominant when energy loss is small
  - High residual energies
  - Low material budget
- Dedicated calibration procedure was performed for each setting (dashed lines)
  - Maximum relative error could be reduced to $\approx \mathcal{O}‰$

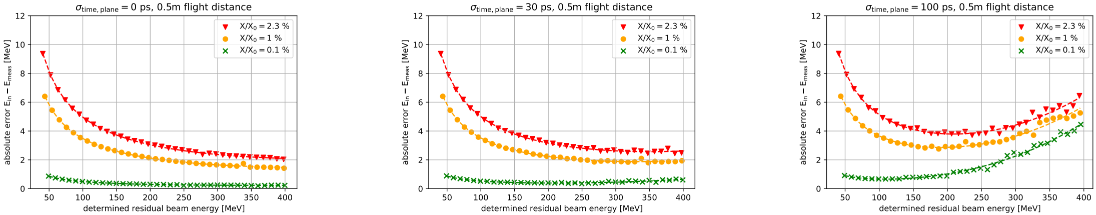

Outline

iCT setup – Overview

Performed simulations

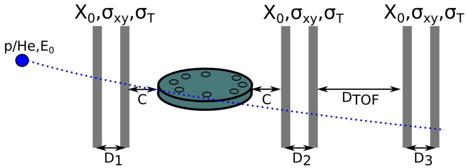

Ion computed tomography setup based on 4D tracking detectors.

- ➛ CTP404 was used for performance studies
- ➛ Primary particle flux: $100\,\text{p}/\text{mm}^2$
- ➛ 360 projection angles in 1 deg steps
- ➛ DDB for reconstruction (Rit et al. 2012)

Parameter	Range	Stepsize
$\mathbf{X}/\mathbf{X_0}$	$0.1 - 2.3\,\%$	$\approx 1\,\%$
$\sigma_{\mathbf{xy}}$	$0\,\mu$m	fixed
$\sigma_{\mathbf{T}}$	$0 - 100$ ps	$10 - 50$ ps
C	10 cm	fixed
$\mathbf{D_{1,2,3}}$	10 cm	fixed
$\mathbf{D_{TOF}}$	$50 - 200$ cm	50 cm
$\mathbf{E_0}$	$200 - 400$ MeV	50 MeV
Particle type	proton	fixed

Summary of the iCT system parameters which were varied to study the overall performance.

iCT setup – Analysis

Catphan Analysis

- RSP values were collected in $6 \times 6\text{mm}^2$ ROIs at each insert (15 slices each)
- Mean absolute percentage error (MAPE) and coefficient of variation (CV) were used for RSP accuracy and precision estimation

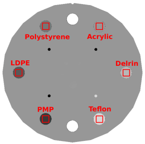

CTP404 phantom (frontal view)

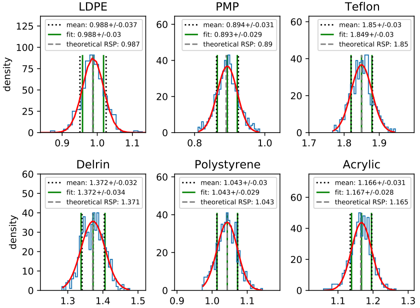

Example RSP distributions for $E_0 = 200$ MeV , $X/X_0 = 0.1\,\%$, $L = 1$ m

$$\mathrm{CV} = \frac{\sigma_{\mathrm{RSP}}}{\mu_{\mathrm{RSP}}}, \quad \mathrm{err_{rel}} = \frac{|\mathrm{RSP_{theo}} - \mathrm{RSP_{meas}}|}{\mathrm{RSP_{theo}}}, \quad \mathrm{MAPE} = \frac{\sum_i^{n_{\mathrm{mat}}} \mathrm{err_{rel,i}}}{n_{\mathrm{mat}}}$$

Outline

Selected results – Precision

RSP precision

- Energy resolution and RSP resolution are mainly dominated by intrinsic time resolution per plane and beam energy
- Central slice for 200 and 400 MeV protons and 0.1 $\% X/X_0$

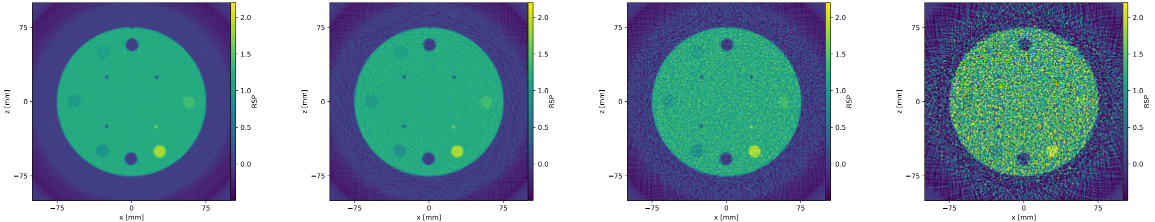

$\sigma_{\text{time,plane}} = 30$ ps, $E_0 = 200$ MeV | $\sigma_{\text{time,plane}} = 100$ ps, $E_0 = 200$ MeV | $\sigma_{\text{time,plane}} = 30$ ps, $E_0 = 400$ MeV | $\sigma_{\text{time,plane}} = 100$ ps, $E_0 = 400$ MeV

Selected results – Precision

RSP precision

Insert	ideal pCT	TOF-pCT$^{30\,\text{ps}}_{0.1\,\%\,\frac{X}{X_0}}$	TOF-pCT$^{30\,\text{ps}}_{1.0\,\%\,\frac{X}{X_0}}$	TOF-pCT$^{30\,\text{ps}}_{2.3\,\%\,\frac{X}{X_0}}$
PMP	2.77	3.479	3.649	3.675
LDPE	2.295	3.118	3.062	3.541
Polystyrene	2.239	2.834	3.01	3.121
Acrylic	1.968	2.636	2.819	3.089
Delrin	1.835	2.308	2.378	2.475
Teflon	1.276	1.64	1.655	2.287

RSP coefficient of variation [%] of the iCT system for 200 MeV protons and a calorimeter length of 1m.

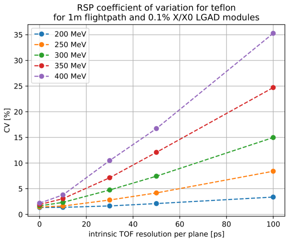

CV measured in teflon insert

- RSP precision could be further improved
  - F.ex.: by adapting calorimeter length or by increasing nr of LGADs per timing layer

Selected results – Precision

RSP precision

Insert	ideal pCT	$\text{TOF-pCT}^{10\,\text{ps}}_{0.1\,\%\,\frac{X}{X_0}}$	$\text{TOF-pCT}^{10\,\text{ps}}_{1.0\,\%\,\frac{X}{X_0}}$	$\text{TOF-pCT}^{10\,\text{ps}}_{2.3\,\%\,\frac{X}{X_0}}$
PMP	2.77	2.705	3.068	3.062
LDPE	2.295	2.501	2.577	2.969
Polystyrene	2.239	2.422	2.494	2.669
Acrylic	1.968	2.136	2.321	2.534
Delrin	1.835	1.858	2.007	2.163
Teflon	1.276	1.367	1.403	1.656

RSP coefficient of variation [%] of the iCT system for 200 MeV protons and a calorimeter length of 1m.

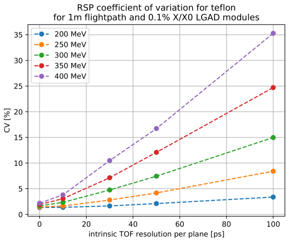

CV measured in teflon insert

- ➛ RSP precision could be further improved
  - ▶ F.ex.: by adapting calorimeter length or by increasing nr of LGADs per timing layer

Selected results – Accuracy

RSP accuracy

- Dedicated calibration procedure for TOF calorimeter was implemented
- After calibration RSP accuracy could be lowered down to ≈ 0.12-0.6 %
  - Well below clinical requirements

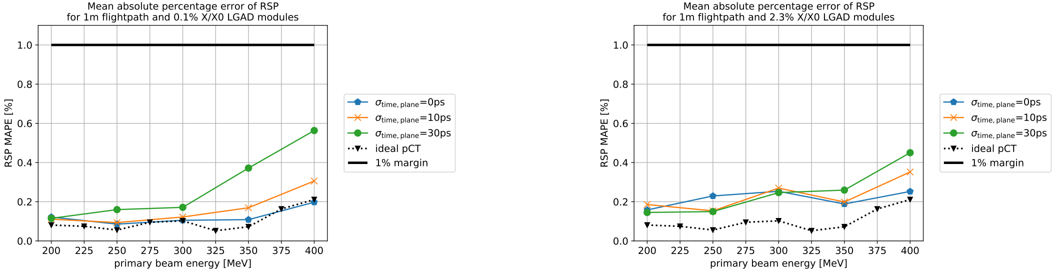

Selected results – Accuracy

RSP accuracy

Insert	$\mathrm{RSP}_{\mathrm{ref}}$	ideal pCT	TOF-pCT$^{30\,\mathrm{ps}}_{0.1\,\%\,\frac{X}{X_0}}$	TOF-pCT$^{30\,\mathrm{ps}}_{1.0\,\%\,\frac{X}{X_0}}$	TOF-pCT$^{30\,\mathrm{ps}}_{2.3\,\%\,\frac{X}{X_0}}$
PMP	0.89	0.232 ± 0.119	0.410 ± 0.150	0.306 ± 0.158	-0.033 ± 0.160
LDPE	0.987	-0.004 ± 0.099	0.098 ± 0.162	0.177 ± 0.132	0.262 ± 0.153
Polystyrene	1.043	-0.030 ± 0.096	0.012 ± 0.122	0.007 ± 0.120	0.211 ± 0.135
Acrylic	1.165	0.035 ± 0.085	0.057 ± 0.113	0.162 ± 0.121	0.154 ± 0.133
Delrin	1.371	-0.330 ± 0.079	0.103 ± 0.099	0.074 ± 0.102	-0.008 ± 0.107
Teflon	1.85	-0.153 ± 0.055	0.011 ± 0.071	-0.007 ± 0.712	-0.202 ± 0.098
MAPE [%]	-	**0.081**	**0.115**	**0.122**	**0.145**

Relative RSP errors [%] of the iCT system for 200 MeV protons and a calorimeter length of 1m. The standard error of the mean was used to estimate the uncertainty of the RSP accuracy in each insert.

Outline

Summary and Outlook

- Design studies for an iCT sytstem based on 4D-tracking detectors were started
  - Multiple system parameters were varied and optimized (based on MC simulations)
  - CTP404 was used to measure RSP precision and accuracy
- An LGAD-based iCT system could potentially fulfill clinical requirements
  - For almost all settings, the RSP MAPE was between 0.12-0.6 %
  - RSP precision and energy resolution can still be improved
- Next steps:
  - Should be verified experimentally
  - Development of an iCT demonstrator based on LGADs is planned

Acknowledgements

Contributors

- Thomas Bergauer
- Alexander Burker
- Albert Hirtl
- Christian Irmler
- Stefanie Kaser
- Florian Pitters

Reconstruction software

- Simon Rit

Thank you for your attention

HEPHY
INSTITUT FÜR HOCHENERGIEPHYSIK

TECHNISCHE UNIVERSITÄT WIEN

Outline

Backup– Intrinsic time resolution of an LGAD

Intrinsic time resolution (Sadrozinski et al. 2017)

$$\sigma_t{}^2 = \sigma_{\mathrm{TimeWalk}}{}^2 + \sigma_{\mathrm{LandauNoise}}{}^2 + \sigma_{\mathrm{Distortion}}{}^2 + \sigma_{\mathrm{Jitter}}{}^2 + \sigma_{\mathrm{TDC}}{}^2$$

- $\sigma_{\mathrm{TimeWalk}}$
  - A constant signal threshold for varying signal amplitudes, but constant rise times, induces an uncertainty in the time-of-arrival and time-over-threshold
- $\sigma_{\mathrm{LandauNoise}}$
  - Statistical fluctuations of energy deposition in active volume of the sensor
- $\sigma_{\mathrm{Distortion}}$
  - Non-uniform weighting field and non-saturated drift velocity $(i(t) = -q\vec{v} \cdot \vec{E_{\mathrm{W}}})$
- σ_{Jitter}
  - Time uncertainty due to early or late firing of the comparator due to noisy signal (depends on gain)
- σ_{TDC}
  - Time uncertainty due to limited time resolution of TDC (binning)

HEPHY INSTITUT FÜR HOCHENERGIEPHYSIK
TU WIEN TECHNISCHE UNIVERSITÄT WIEN

Backup – Tracker

Tracking telescope with 2+2 DSSDs

- DSSD
  - Thickness: 300 µm
  - Size: $(2.56 \times 5.12)\,\text{cm}^2$
    - X-side: 512 p-doped strips with 50 µm pitch
    - Y-side: 512 n-doped strips with 100 µm pitch
- GbE-based readout
  - APV25 chip (French et al. 2001)
  - Belle-II SVD readout chain with adapted FW and SW (Thalmeier et al. 2017)
  - Achieved event-rate $\leq 30\,\text{kHz}$
- Corryvreckan framework for tracking (Dannheim et al. 2021)
  - Detector alignment
  - Track fitting
  - Phantom positioning based on MCS radiography (Schütze et al. 2018)

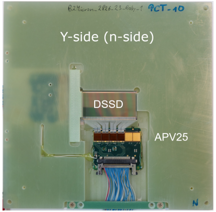

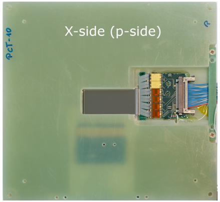

Backup – Tracker readout system

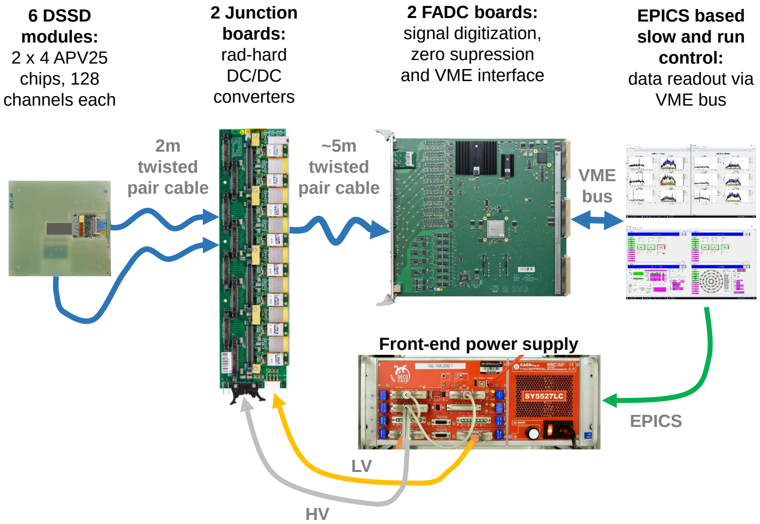

Backup – Calorimeter

Implementation of a range telescope (formerly TERA (Bucciantonio et al. 2013))

- 42 plastic scintillators layers
  - Size: $(3 \times 300 \times 300)\,\text{mm}^3$ (≈ 3.6 mm WET)
  - Can measure protons up to ≈ 150 MeV
- SiPMs for signal generation
  - 400 pixel
  - Subsequent ADC resolution (12 bit)
  - Limited energy range
    - Range telescope instead of sampling calorimeter
- Readout via USB connection
  - Event rate < 16 kHz
- SiPM power supply was unstable
  - Mainboard was completely redesigned

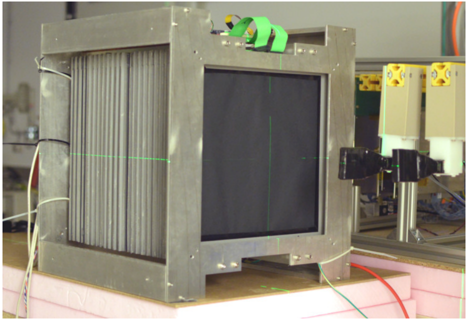

Backup – SiPM calibration

- SiPM operates in Geiger mode
  - Light from scintillators is measured with SiPMs
  - Signal is proportional to number of detected photons (fired pixels) $\rightarrow \mathrm{E}_{\mathrm{dep}}$ in scintillator
- Limited energy range and resolution
  - Only 400 pixel
  - Subsequent ADC resolution (12 bit)
- Energy deposition in scintillator $\propto$ Landau distribution
  - MPV is shifted by adapting bias voltage (gain) to optimise energy range and energy resolution
    - ★ Gain very sensitive to voltage instabilities and temperature
  - MPV of ADC counts is then converted to deposited energy by comparison to Geant4 simulation (calibration)

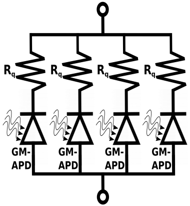

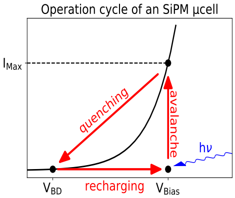

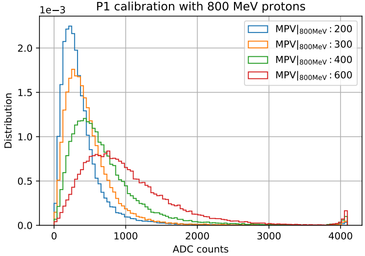

Backup – Calorimeter calibration

- Optimization of SiPM dynamic range
  - SiPM calibration was performed with 800 MeV protons at MedAustron
- Calibration of range telescope
  - Estimation of mean water equivalent thickness (WET) of the calorimeter components
    - Ranges are measured for different proton energies
    - Comparison to NIST data for WET estimation of trigger scintillators and TERA scintillators
- Range algorithm for single protons
  - Energy cuts in plateau (pile-ups)
  - Last slice over threshold and first slice under threshold defines range
    - To compensate fluctuations of single slices

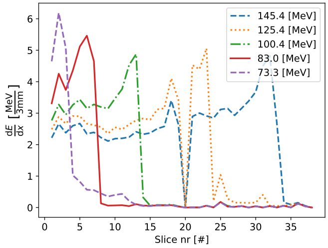

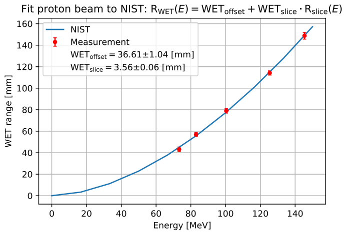

Backup – Testbeam at MedAustron

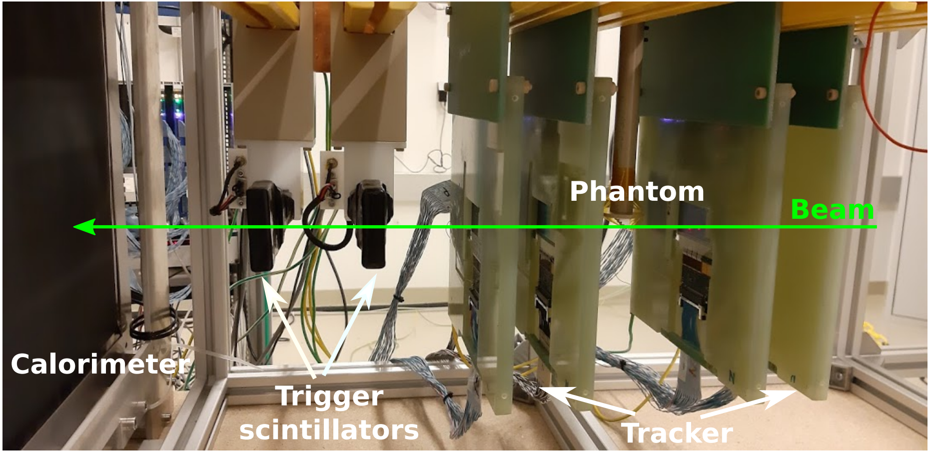

Accelerator layout

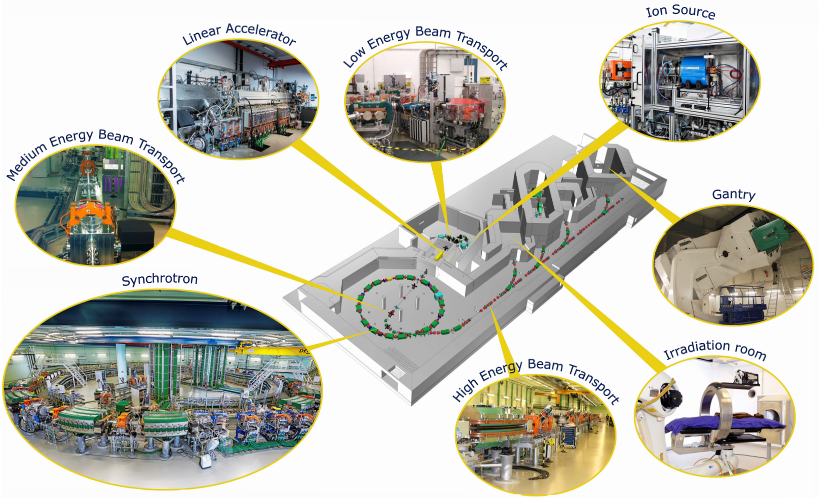

Image: MedAustron

Accelerator layout – Synchrotron

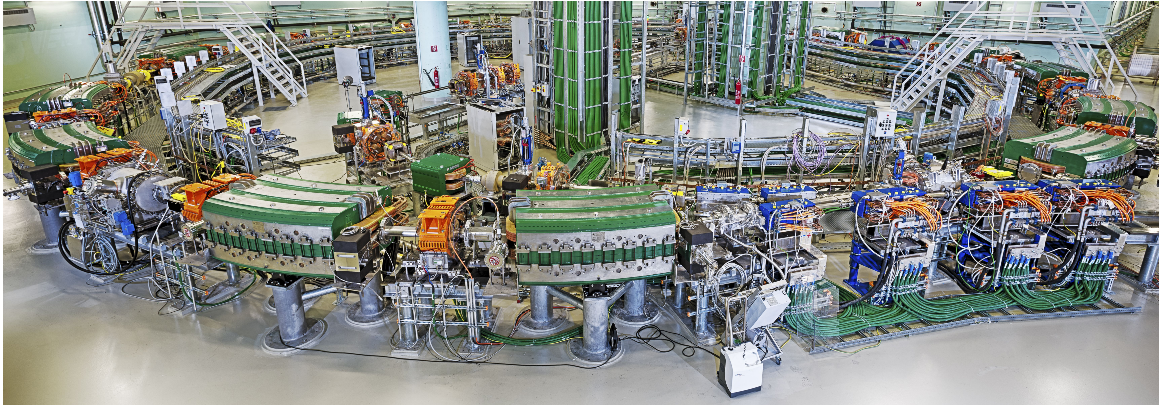

Image: MedAustron

- circumference 78 m
- radius 12 m
- 16 dipole magnets
- 24 quadrupole magnets
- 1 RF cavity for acceleration

Backup– MedAustron

Synchrotron accelerator complex

- Circumference: 77.4 m
- Energies:
  - Protons: 60 MeV to 800 MeV, Clinical energies $\leq$ 250 MeV
  - Carbon ions: 120 MeV/u to 400 MeV/u

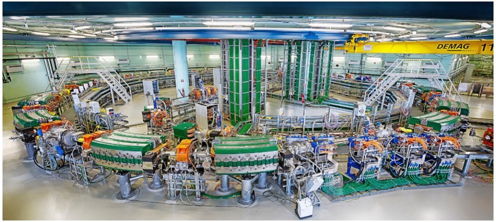

- 4 slots for ion sources:
  - Protons
  - Carbon ions
  - Redundant source
  - Unused, could be used for He

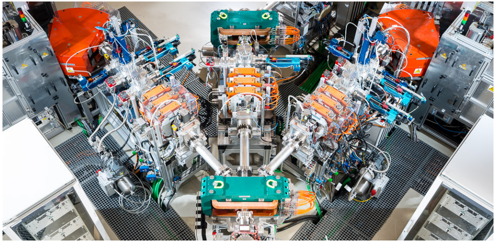

HEPHY INSTITUT FÜR HOCHENERGIEPHYSIK

TU WIEN TECHNISCHE UNIVERSITÄT WIEN

Backup– MedAustron

Synchrotron accelerator complex

- Four irradiation rooms:
  - IR1: **Exclusive to research**
    (protons up to 800 MeV, low rates)
  - IR2, IR3, IR4: Clinical use
    (Limited to clinical energies)
  - Beam only in one room at a time
- **Beam parameters:**
  - Beam delivery: pencil beam scanning
  - 5 s spill
  - Spotsize: 7 mm to 21 mm FWHM
  - Clinical rates:
    - Protons: 10^9 particles/s
    - Carbon ions: 10^7 particles/s
  - Research: $\geq 10^3$ particles/s

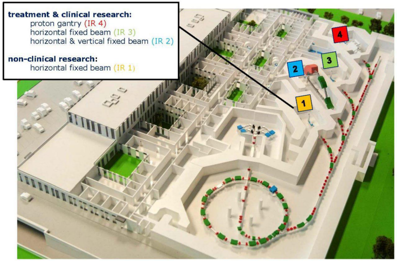

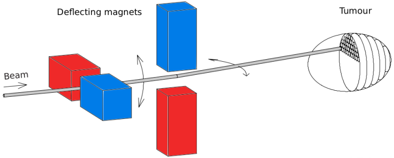

Backup – TIGRE toolbox

- **TIGRE: Tomographic Iterative GPU-based Reconstruction Toolbox**
- Developed for cone beam CT (CBCT)
  - Used by collaborating group at MedUni Vienna for CBCT
- Single or multi-GPU computation
- Modular structure
- Forward and backprojection ($A(x)$) are optimized for GPU computing
- Algortihms are written in high-level language (Python, Matlab)

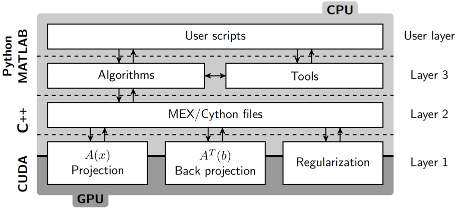

Image: TIGRE (Biguri et al. 2016)

- Available algorithms:
  - Filtered back projection, FDK
  - Iterative algorithms (SART, OS-SART,..)
  - Custom algorithms

[7] https://arxiv.org/abs/1905.03748

References I

Bashkirov, V. A. et al. (Jan. 2016). "Novel scintillation detector design and performance for proton radiography and computed tomography". In: *Medical Physics* 43.2, pp. 664–674. DOI: 10.1118/1.4939255.

Biguri, Ander et al. (2016). "TIGRE: a MATLAB-GPU toolbox for CBCT image reconstruction". In: *Biomedical Physics & Engineering Express* 2.5, p. 055010. DOI: 10.1088/2057-1976/2/5/055010.

Bucciantonio, M. et al. (2013). "Development of a fast proton range radiography system for quality assurance in hadrontherapy". In: *Nuclear Instruments and Methods in Physics Research Section A: Accelerators, Spectrometers, Detectors and Associated Equipment* 732. Vienna Conference on Instrumentation 2013, pp. 564 –567. ISSN: 0168-9002. DOI: 10.1016/j.nima.2013.05.110.

Collins-Fekete, Charles-Antoine et al. (Apr. 2020). "Statistical limitations in proton imaging". In: *Physics in Medicine & Biology* 65.8, p. 085011. DOI: 10.1088/1361-6560/ab7972.

Dannheim, D. et al. (2021). "Corryvreckan: a modular 4D track reconstruction and analysis software for test beam data". In: *Journal of Instrumentation* 16.03, P03008. DOI: 10.1088/1748-0221/16/03/p03008.

French, M.J. et al. (2001). "Design and results from the APV25, a deep sub-micron CMOS front-end chip for the CMS tracker". In: *Nuclear Instruments and Methods in Physics Research Section A: Accelerators, Spectrometers, Detectors and Associated Equipment* 466.2. 4th Int. Symp. on Development and Application of Semiconductor Tracking Detectors, pp. 359 –365. ISSN: 0168-9002. DOI: 10.1016/S0168-9002(01)00589-7.

Pietraszko, J. et al. (July 2020). "Low Gain Avalanche Detectors for the HADES reaction time (T$$_0$$) detector upgrade". In: *The European Physical Journal A* 56.7. DOI: 10.1140/epja/s10050-020-00186-w. URL: https://doi.org/10.1140/epja/s10050-020-00186-w.

References II

Pitters, Florian et al. (2020). "Ion Beam Imaging Activities at TU Wien and HEPHY". talk at Loma Linda Workshop 2020. URL: http://ionimaging.org/talks/ws2020llu-florian-pitters/.

Rit, S. et al. (2012). "Distance-driven binning for proton CT filtered backprojection along most likely paths". In: URL: https://www.creatis.insa-lyon.fr/~srit/biblio/rit2012b.pdf.

Rovituso, M et al. (2017). "Fragmentation of 120 and 200 MeV u-14He ions in water and PMMA targets". In: *Physics in Medicine and Biology* 62.4, pp. 1310–1326. DOI: 10.1088/1361-6560/aa5302.

Sadrozinski, Hartmut F-W et al. (2017). "4D tracking with ultra-fast silicon detectors". In: *Reports on Progress in Physics* 81.2, p. 026101. DOI: 10.1088/1361-6633/aa94d3.

Schütze, Paul et al. (2018). "Feasibility Study of a Track-Based Multiple Scattering Tomography". In: *Proceedings of International Conference on Technology and Instrumentation in Particle Physics 2017*. Ed. by Zhen-An Liu. Singapore: Springer Singapore, pp. 164–170. ISBN: 978-981-13-1316-5. DOI: 10.1063/1.5005503.

Thalmeier, R. et al. (2017). "The Belle II SVD data readout system". In: *Nuclear Instruments and Methods in Physics Research Section A: Accelerators, Spectrometers, Detectors and Associated Equipment* 845. Proceedings of the Vienna Conference on Instrumentation 2016, pp. 633 –638. ISSN: 0168-9002. DOI: https://doi.org/10.1016/j.nima.2016.05.104.

Ulrich-Pur, Felix et al. (2021). *A Proton Computed Tomography Demonstrator for Stopping Power Measurements*. arXiv: 2106.12890 [physics.med-ph].